Water Practice & Technology

IWA PUBLISHING

Water Practice & Technology Vol 16 No 4, 1410 doi: 10.2166/wpt.2021.078

Adsorption of vanadium with amorphous hydrated chromium oxide

Hualin Li[a,b,d], Hongling Zhang [a,b,c,*], Minting Luo[a,b], Yuming Dong[a,b], Hongbin Xu[a,b,c], Xichuan Cheng[e] and Zaihua Cai[e]

[a] CAS Key Laboratory of Green Process and Engineering, Institute of Process Engineering, Chinese Academy of Sciences, Beijing 100190, China
[b] National Engineering Laboratory for Hydrometallurgical Cleaner Production Technology, Institute of Process Engineering, Chinese Academy of Sciences, Beijing 100190, China
[c] University of Chinese Academy of Sciences, Beijing 100049, China
[d] Beijing BOE Display Technology Co., Ltd, Beijing 101100, China
[e] Hubei Zhenhua Chemical Co. Ltd, Huangshi 435001, China
*Corresponding author. E-mail: hlzhang@ipe.ac.cn

HZ, 0000-0002-9544-3933

ABSTRACT

Vanadium is recognized as a potentially dangerous pollutant following closely behind lead, mercury and arsenic. Vanadium removal from wastewater prior to discharge is essential. In this work, an amorphous hydrated chromium oxide was prepared and its vanadium adsorption ability studied. As prepared, the hydrated oxide showed high efficiency in vanadium adsorption – e.g., from 300 to 0.75 mg-V·L^{-1}. The effects of pH, adsorbent dosage, temperature, adsorption time and the presence of other ions on the vanadium removal rate were investigated, and optimal parameters determined. Dynamic adsorption results showed that pseudo-second-order kinetics could be used to interpret the kinetic curve and that the process was that of chemisorption. The Langmuir isotherm was found to fit the adsorption behavior well.

Key words: adsorption, hydrated chromium oxide, vanadium-containing wastewater, vanadium removal

HIGHLIGHTS

- An amorphous hydrated chromium oxide was used for vanadium adsorption.
- The concentration of vanadium ions could be decreased from 300 to 0.75 mg·L^{-1}.
- Effects of parameters and adsoption kinetics and isotherms were studied.
- Common co-existing ions show little influence on the adsorption efficiency.

INTRODUCTION

The continued expansion of application fields and market demands is leading to rapid development of the vanadium industry (Khalid *et al.* 2017). Meanwhile, large amounts of vanadium-containing wastewater have been produced. Vanadium is toxic and can exist in three valence states – +3, +4 and +5 – in aqueous solution, of which +5 is the most stable (Kong *et al.* 2020). The +5 oxidation state is also the most toxic of the three (Yu & Yang 2019). Vanadium is recognized as a potentially dangerous pollutant following closely behind lead, mercury and arsenic (Naeem *et al.* 2007) so it is essential to remove vanadium ions from wastewater prior to discharge.

Various methods have been investigated for vanadium removal from vanadium-containing wastewater, etc, including chemical precipitation (Xiong *et al.* 2018), ion exchange (Hu *et al.* 2009), solvent extraction (Wang *et al.* 2021), adsorption (Li *et al.* 2014; Padilla-Rodríguez *et al.* 2015; Peng *et al.* 2017), and so on. Comparatively, adsorption has been used widely as it is highly effective, inexpensive, simple to operate and has high adsorption efficiency (Padilla-Rodríguez *et al.* 2015; Peng *et al.* 2017). Adsorption performance is closely related to the adsorbent's physicochemical characteristics (Hong *et al.* 2019). An adsorbent should have high adsorption capacity and depth, so that the vanadium concentration in the treated wastewater meets the vanadium discharge standard (e.g., $<$1.0 mg-V·L^{-1}, State Administration for Quality Supervision, Inspection and Quarantine, Ministry of Environmental Protection, People's Republic of China 2011).

Vanadium and chromium are in ores such as vanadium titano-magnetite, chromite, etc (Yang *et al.* 2020), so chromium could also be recovered in vanadium industry wastewater. As a result, use of a chromium compound for vanadium removal might be feasible.

Hydroxides have been reported for the adsorption of vanadium, chromium, phosphate, etc. (Naeem *et al.* 2007; Cheng *et al.* 2011; Li *et al.* 2014). A sample with enhanced crystallinity was reported as having a significantly smaller specific surface and poor adsorption capacity (Cheng *et al.* 2011), indicating the advantage of using amorphous adsorbents.

In this study, an amorphous hydrated chromium oxide was prepared via a hydrogen reduction method (Bai *et al.* 2006; Liang *et al.* 2020), its structure, specific surfaces and porosities characterized, and its vanadium adsorption properties, as prepared, studied. Variations in pH, adsorbent dosage, temperature, time, common co-existing ions and desorption efficiency were investigated. Appropriate kinetic and equilibrium models were applied to gain insight into vanadium adsorption characteristics.

MATERIALS AND METHODS

Materials

Analytical grade potassium chromate (K_2CrO_4), sodium metavanadate ($NaVO_3{\cdot}2H_2O$), hydrochloric acid (HCl), sodium hydroxide (NaOH), sodium nitrate ($NaNO_3$), sodium sulfate (anhydrous, Na_2SO_4), sodium chloride (NaCl), potassium chloride (KCl), magnesium chloride (MgCl) and sodium chloride (anhydrous, $CaCl_2$) were purchased from Sinopharm Chemical Reagent Co., Ltd (China). The hydrogen gas, purchased from Praxair Inc, was 99.99% pure by volume. All solutions used were prepared with deionized water.

Synthesis and characterization of hydrated chromium oxide

Amorphous hydrated chromium oxide was prepared by hydrogen reduction. The heating apparatus, a tube stove with programmable temperature controller, was used as the reactor for the gas-solid reductive reaction. A nichrome boat loaded with potassium chromate was put into the sealed tube stove and hydrogen was introduced to form a reducing atmosphere. The stove was heated to 450 °C and kept at that temperature for 1.0 hour, before cooling naturally to ambient temperature. The resulting product was washed several times until all soluble components were removed completely. Finally, the washed product was dried at 80 °C for 24.0 hours.

X-ray diffraction (XRD) and Fourier transform infrared spectrometry (FT-IR) were used to determine the phases and structure of the sample. The XRD analysis was carried out with a Rigaku diffractometer in 2θ range 5 to 90° using CuKα radiation. The FT-IR spectra were recorded with a Spectra GXFT-IR Spectrometer with scan number 8 and 4 cm^{-1} resolution. Field emission scanning electron microscope (SEM) (JSM-7610F) image analysis was carried out with15.0 kV accelerating voltage. BET specific surface and pore size distribution were tested using nitrogen adsorption and desorption in a physical and chemical adsorption instrument (NOVA3200e).

Adsorption experiments

Batch adsorption studies were conducted to determine the equilibrium time to reach saturation. Typically, 20 mL of 300 mg-V·L^{-1} vanadium ion solution was mixed with a known dose of adsorbent in 50 mL vials (oscillation 180 r·min^{-1}). All experiments were performed in triplicate, and the parameters varied in the study were initial pH (1.0 to 13.0), adsorbent dose (n_{Cr}:n_V) (6:1 to 90:1), temperature (25 to 60 °C) and contact time (0.17 to 24.0 hr). The solution pH was adjusted by adding HCl or NaOH.

At preplanned times, samples were separated by filtration and analyzed by inductively coupled plasma atomic emission spectrometry (Optima 5300 DV – Perkin-Elmer, USA). The amount of vanadium adsorbed was evaluated as the difference between the initial and residual concentrations. Adsorption efficiency was calculated using Equation (1):

$$Adsorption(\%) = \frac{C_0 - C_t}{C_0} \times 100 \quad (1)$$

where C_0 is the initial vanadium concentration (mg-V·L^{-1}); and C_t the residual vanadium concentration (mg-V·L^{-1}) at time t.

The adsorbent's adsorption capacity at time t, q_t (mg·g^{-1}) was calculated using Equation (2):

$$q_t = \frac{V(C_0 - C_t)}{W} \tag{2}$$

where V is the solution volume (L); and W the adsorbent dosage (g).

The effects of common co-existing ions were studied in mixed solutions with an initial vanadium concentration of 500 mg-V·L^{-1}, and the co-existing ions varied from 100 to 500 mg·L^{-1}. The experimental conditions adopted with the co-existing ions were initial pH 2.0, adsorbent dosage (n_{Cr}:n_V) 60:1, 30 °C and 10.0 hours.

Adsorption kinetics

The adsorption kinetics study was carried out at 30, 40 and 50 °C, with an initial vanadium concentration of 300-V mg·L^{-1} for different times. The results were analyzed using the pseudo-first-order and pseudo-second-order models (Ho *et al.* 2000; Li *et al.* 2014), described by Equations (3) and (4):

$$\log(q_e - q_t) = \log q_e - \frac{k_1}{2.303}t \tag{3}$$

$$\frac{1}{q_t} = \frac{1}{k_2 q_e^2}\cdot\frac{1}{t} + \frac{1}{q_e} \tag{4}$$

where q_e is the equilibrium adsorption capacity, q_t the adsorption capacity at time t, and k_1 and k_2 the reaction rate constants for the pseudo-first-order *and* pseudo-second-order models.

Adsorption isotherms

The adsorption isotherm study was carried out at 30, 40 and 50 °C with the initial vanadium concentration varied from 100 to 500 mg·L^{-1} for 10 hours. The results were analyzed using the Langmuir and Freundlich empirical models (Naeem *et al.* 2007), described by Equations (5) and (6):

$$\text{Langmuir: } \frac{1}{q_e} = \frac{1}{q_m k_L C_e} + \frac{1}{q_m} \tag{5}$$

$$\text{Freundlich: } \log q_e = \frac{1}{n}\log C_e + \log k_F \tag{6}$$

where q_e is the equilibrium adsorption capacity, q_m the maximum adsorption capacity, k_L the Langmuir constant related to the adsorption capacity, C_e the vanadium concentration in solution, and k_F and $\frac{1}{n}$ Freundlich constants related to adsorption capacity and intensity, respectively.

RESULTS AND DISCUSSION

Characterizations of the hydrated chromium oxide

The FT-IR spectrum of the as-prepared sample – range 400 to 4,000 cm^{-1}, resolution 1 cm^{-1} – is presented in Figure 1, and shows major peaks at 3,375, 2,017, 1,635, 835 and 505 cm^{-1}. The strong adsorption peak at 505 cm^{-1} relates to Cr(III)-O antisymmetric stretching vibration, and that at 835 cm^{-1} to Cr(III)-O-H bending vibration (Yang *et al.* 2011). The peak at 1,635 cm^{-1} is caused by bending vibrations in free water molecules. The band corresponding to 1,700 to 2,100 cm^{-1} is the H-O-H stretching vibration (Ratnasamy & Leonard 1972). The other peaks, at 2,800 to 3,500 cm^{-1}, arise from OH stretching on the water surface, which originate in the chemical adsorption of water dissociation (Ratnasamy & Leonard 1972). These characteristic peaks indicate that the sample is γ-CrOOH (Bai *et al.* 2006; Liang *et al.* 2020).

Figure 2 shows the XRD pattern and SEM image of the sample. Only weak diffraction peaks can be seen in the XRD pattern (Figure 2(a)), indicating that the sample is amorphous. In the SEM image (Figure 2(b)), the sample exhibits some lamination and is stacked into irregular agglomerates.

To determine the sample's specific surface and porosity, N_2 adsorption and desorption analysis was carried out. Figure 3(a) and (b) present the N_2 adsorption/desorption isotherms and pore size distribution of the sample, respectively. The hysteresis loop in the isotherms (Figure 3(a)) is typical type H4 (IUPAC classification), indicating the presence of meso- and micro-pores associated with capillary condensation (Thommes *et al.* 2015). In

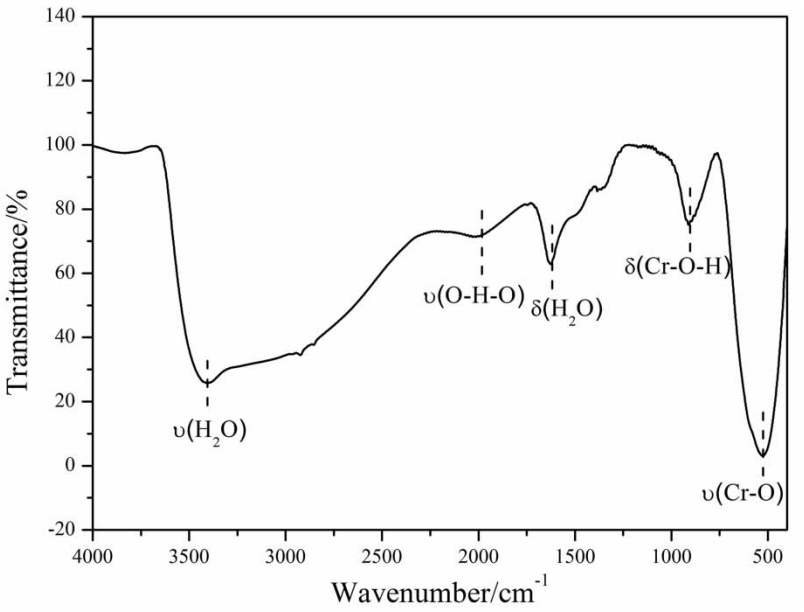

Figure 1 | FT-IR spectrum of the hydrated chromium oxide sample.

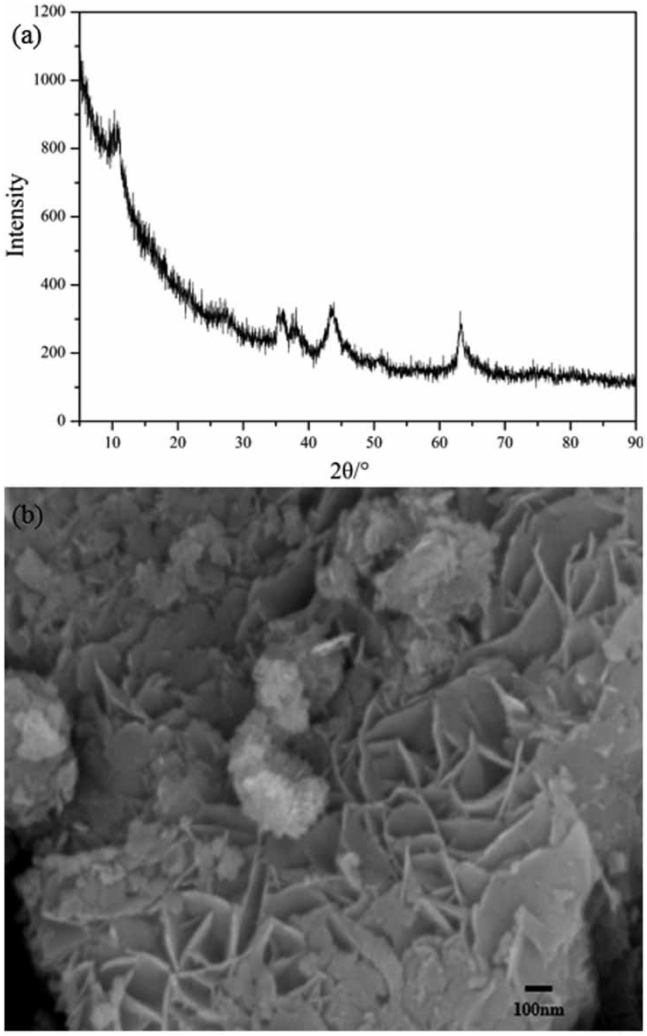

Figure 2 | (a) XRD pattern and (b) SEM image of the hydrated chromium oxide sample.

Figure 3(b), the pore size distribution curve shows a broad peak between about 10 and 50 nm with a maximum at 30 nm. The BET analysis thus indicates that the as-prepared γ-CrOOH is a typical mesoporous material with 99.2 $m^2 \cdot g^{-1}$ specific surface and 0.2 $cm^3 \cdot g^{-1}$ pore volume.

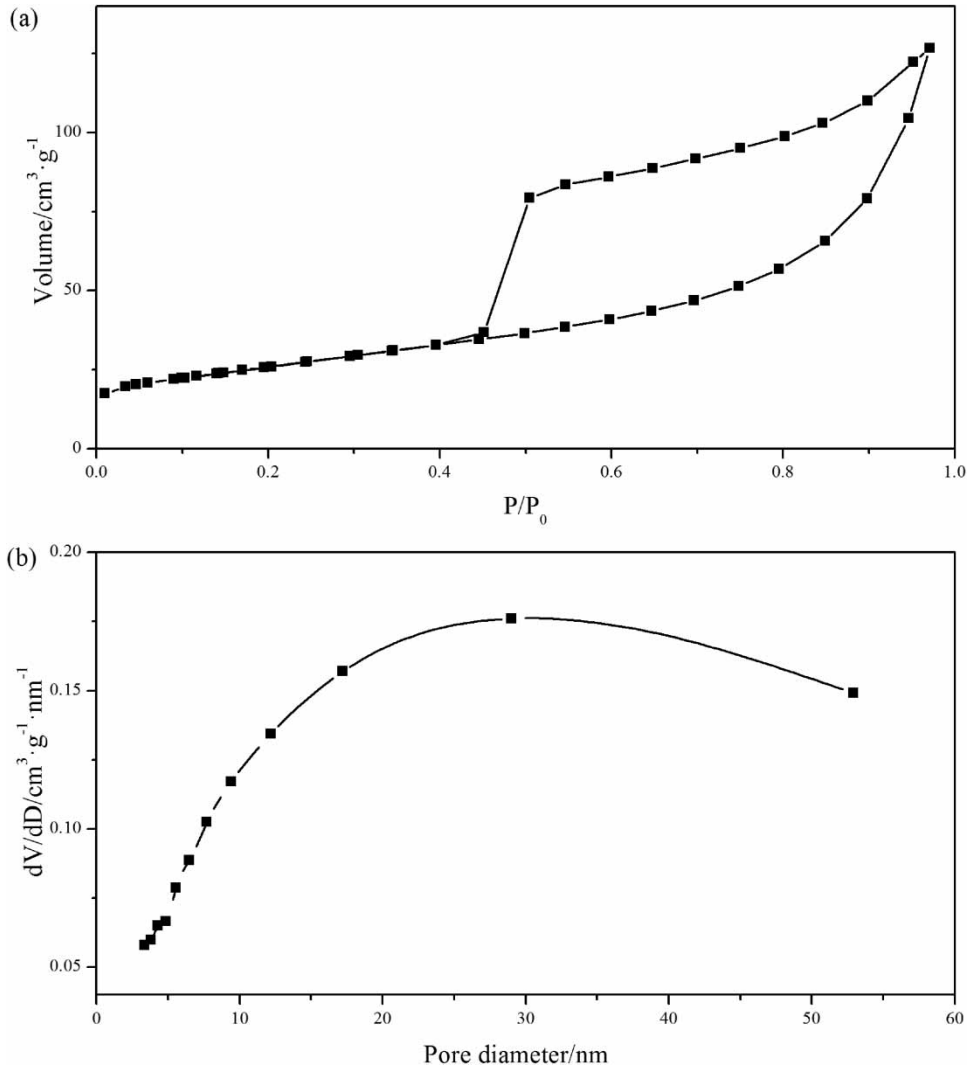

Figure 3 | (a) Nitrogen adsorption/desorption isotherm and (b) BJH pore size distribution plot of the sample.

Effect of pH

Metal ion adsorption on the adsorbent can be affected by the solution's initial pH. Twelve vanadium species can coexist in solution (Sharififard & Rezvanpanah 2021). The cationic species VO_2^+ exists mainly at pH $\leq$2.0, the anionic species, such as decavanadates and other mono- or poly-vanadates, mainly at higher pHs (Li *et al.* 2014). The initial solution pH was adjusted between 1.0 and 13.0 with HCl and NaOH solutions. The adsorption test results are shown in Figure 4.

The solution's initial pH affects the extent of vanadium adsorption onto γ-CrOOH strongly, in behavior typical of metal cation adsorption. Adsorption efficiency increases from pH 1.0 to 2.0 – maximum efficiency is about pH 2.0 – and decreases as the pH increases from 3.0 to 13.0. This is likely associated with competition between H^+ and VO_2^+ for available surface sites (Li *et al.* 2014). Extreme acidity (pH <2.0) makes vanadium adsorption unfavorable, with negligible adsorption at pH 1.0. The sharp decrease in adsorption at pH $\geq$ 3.0 may arise because vanadium ions exist mainly as anionic species in that pH range rather than cations, which are the optimum for adsorption (Sharififard & Rezvanpanah 2021). Thus maximum vanadium adsorption occurs at pH 2.0.

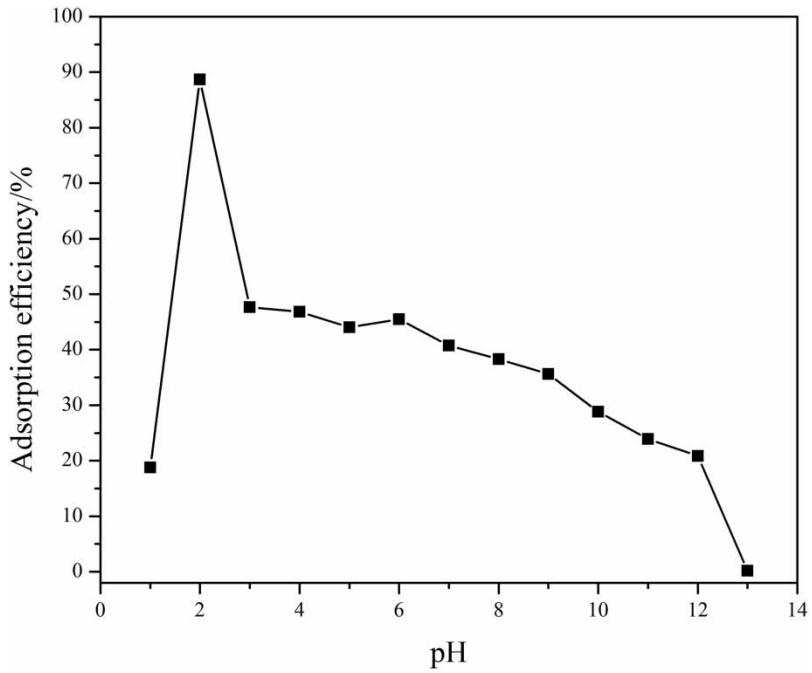

Figure 4 | Vanadium adsorption by γ-CrOOH as a function of pH (300 mg-V·L^{-1}, 25 °C, adsorbent dosage ratio 40:1, 24 hr).

Effect of adsorbent dosage

A series of molar proportions (n_{Cr}:n_V) were selected as adsorbent reference doses on the basis of the vanadium concentration in solution, and the vanadium adsorption efficiency was determined at pH 2.0. As shown in Figure 5, vanadium adsorption efficiency depends strongly on the adsorbent dosage, increasing from 19 to 98% as the molar ratio increases from 6:1 to 90:1. When the ratio is below 60:1, adsorption efficiency increases linearly to 88.14%; above that, it increases more slowly. This is thought to result from the increasing adsorbent dosage, providing more adsorption sites and making the efficiency improve gradually. It can be confirmed that the appropriate adsorbent dosage ratio is 60:1.

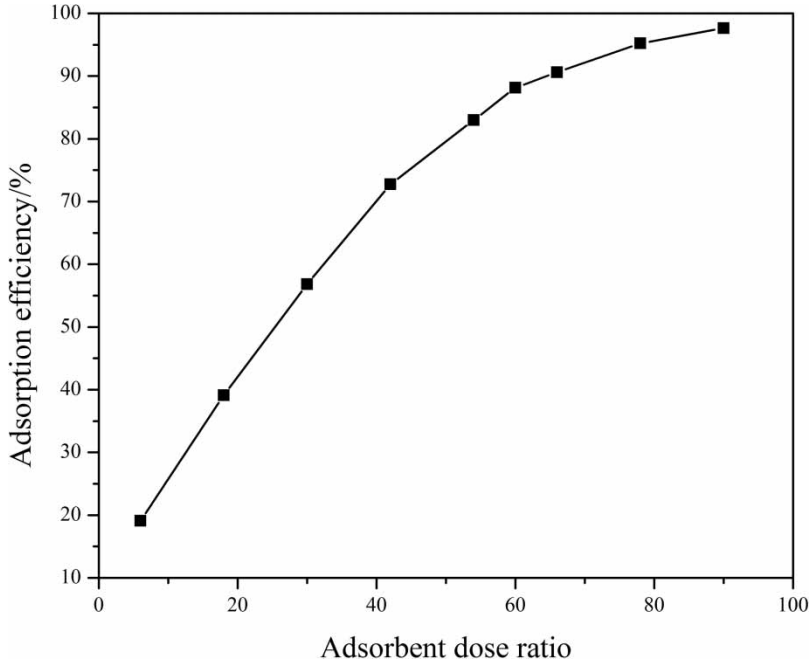

Figure 5 | Vanadium adsorption by γ-CrOOH as a function of adsorbent dose (300 mg-V·L^{-1}, pH 2.0, 25 °C, 24 hr).

Effect of temperature

The effect of temperature was investigated in the range 25 to 60 °C (Figure 6). It is noted that vanadium adsorption increases with increasing temperature, although, at 30 °C and above, the increases are slight and the capacity remains around 9.60 mg·g^{-1}. The vanadium adsorption efficiencies are all close to 100%, however, and the concentration is reduced to <1.0 mg-V·L^{-1}. This indicates that higher temperatures favor the process and that it is endothermic (Salehi *et al.* 2020), and may be because the temperature rise increases the pore size of γ-CrOOH and more surface active sites are available. It may also be that the rates of molecular motion and mass transfer are speeded up by the temperature rise. When the temperature reaches about 30 °C, however, the number of γ-CrOOH surface active sites has reached its maximum and/or the molecular movement rate is at its maximum, making further adsorption capacity increases occur slowly (Li *et al.* 2014).

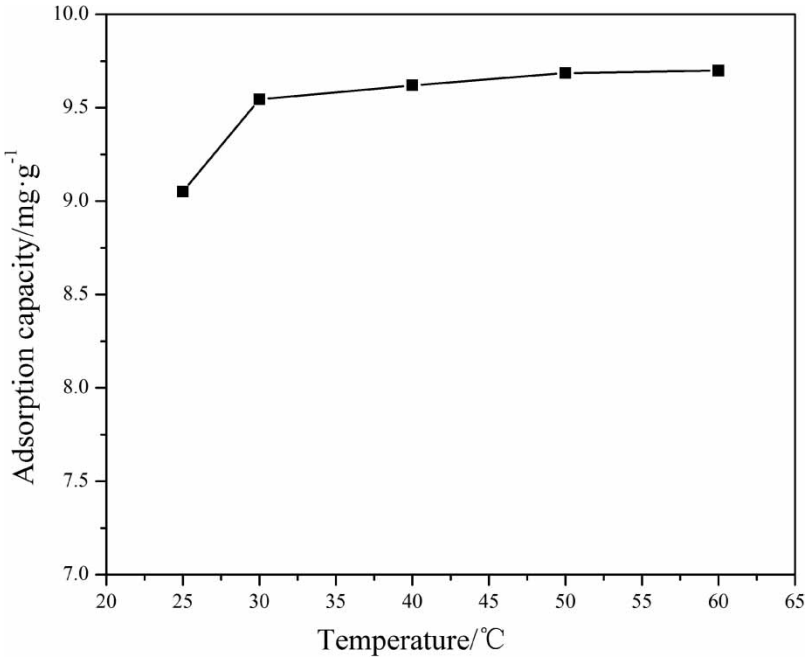

Figure 6 | Vanadium adsorption by γ-CrOOH as a function of temperature (300 mg-V·L^{-1}, pH 2.0, adsorbent dosage ratio 60:1, 24 hr).

Effect of adsorption time

The equilibration time between vanadium and the γ-CrOOH adsorbent was determined by varying the contact time between 0.17 and 24.0 hours, keeping the initial pH and adsorbent dosage ratio constant at 2.0 and 60:1, respectively. Vanadium adsorption rates at different contact times are shown in Figure 7. The rate of vanadium adsorption onto γ-CrOOH increases quickly at first but slightly after 4.0 hours. More than 99% vanadium removal is achieved after 3.0 hours. After 10.0 hours contact, the vanadium concentration is 0.75 mg·L^{-1}; this means no further adsorption occurred. So 10.0 hours can be considered the equilibrium time.

Effect of co-existing ions

The effects of common ions in wastewater, whether anions or cations, such as NO_3^-, SO_4^{2-}, Cl^-, Na^+, K^+, Mg^{2+} and Ca^{2+} were studied (Salehi *et al.* 2020). The concentration of the co-existing ions was varied between 100 and 500 mg·L^{-1}, but the initial vanadium concentration was always 500 mg·L^{-1}. The other experimental conditions were initial pH 2.0, adsorbent dosage (n_{Cr}:n_V) 60:1, 30 °C and 10.0 hours – see Figure 8. There is no obvious effect from the presence of the other ions on vanadium adsorption efficiency. In all of this set of trials the adsorption efficiencies exceeded 97%, showing that γ-CrOOH can remove vanadium from real effluents.

Adsorption kinetics

To determine the dynamics of vanadium adsorption onto γ-CrOOH, adsorption kinetic experiments were carried out. Two kinetic models – pseudo-first-order and pseudo-second-order – were used to analyze the data (Ho *et al.* 2000; Li *et al.* 2014). The fitting data from the two plots are shown in Table 1, which shows that the pseudo-

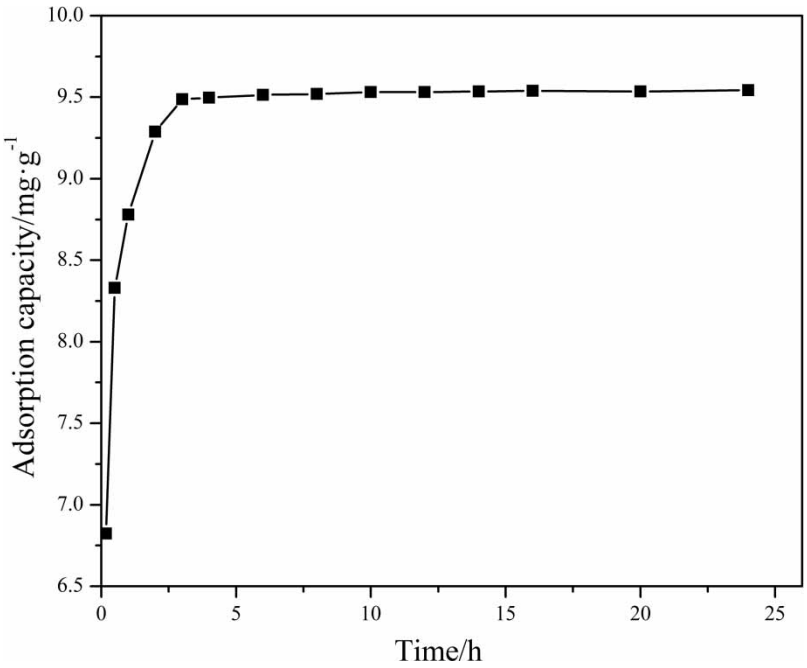

Figure 7 | Vanadium adsorption by γ-CrOOH as a function of time (300 mg-V·L^{-1}, pH 2.0, adsorbent dosage ratio 60:1, 30 °C).

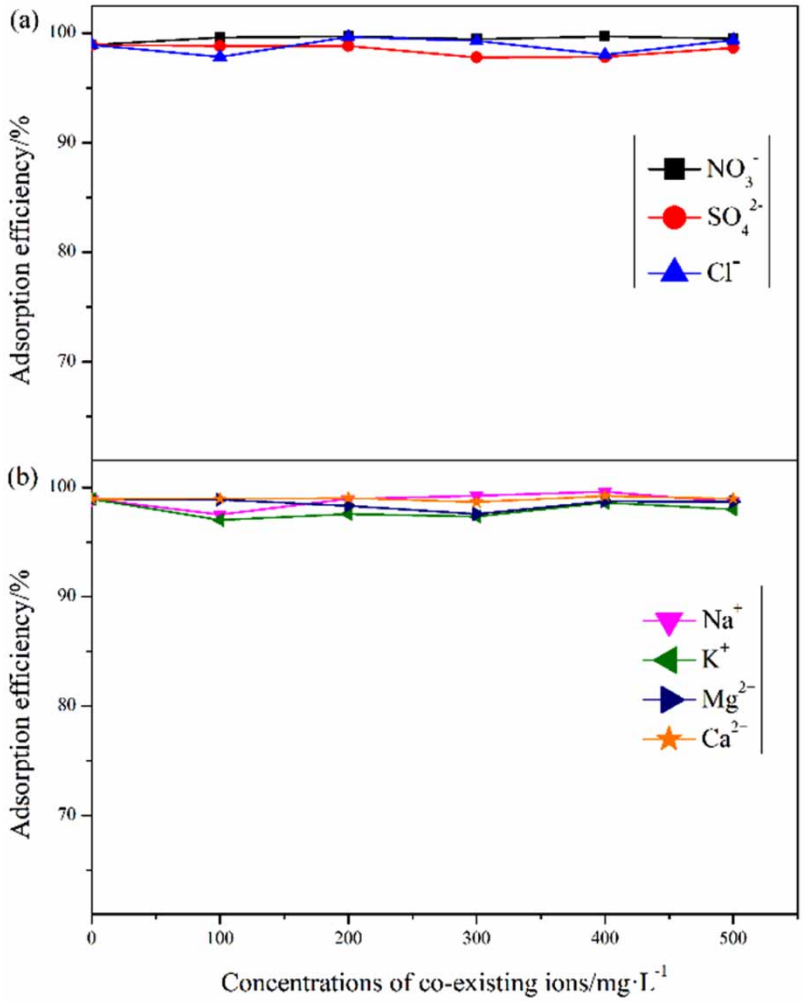

Figure 8 | Influence of common anions (a) and cations (b) on vanadium adsorption by γ-CrOOH (500 mg-V·L^{-1}, pH 2.0, adsorbent dosage ratio 60:1, 30 °C, 10.0 hours).

Table 1 | Parameters of pseudo-first-order and pseudo-second-order models for vanadium adsorption onto γ-CrOOH

Initial vanadium concentration (mg·L^{-1}) 300	T(°C)	Pseudo-first-order			Pseudo-second-order		
		q_e(mg·g^{-1})	k_1(h^{-1})	R^2	q_e(mg·g^{-1})	k_2(h^{-1})	R^2
	30	1.94	0.2747	0.949	9.77	0.9055	0.994
	40	0.25	0.1538	0.779	9.83	7.5539	0.986
	50	0.98	0.2709	0.842	9.86	1.0855	0.986

second-order equation is the more appropriate with R^2 values between 0.986 and 0.994. The pseudo-second-order equation can thus be used to describe the adsorption process, which indicates that the limiting factor for vanadium adsorption onto γ-CrOOH is the chemisorption process (Xie *et al.* 2020).

Adsorption isotherms

The empirical equations of the Langmuir and Freundlich models are the most widely employed in analyzing adsorption processes (Naeem *et al.* 2007). The two parameter sets are listed in Table 2.

Table 2 | Langmuir and Freundlich parameters for vanadium adsorption onto γ-CrOOH (vanadium concentration varied from 100 to 500 mg-V·L^{-1})

	Langmuir			Freundlich		
T(°C)	q_m (mg·g^{-1})	k_L (L·mol^{-1})	R^2	$\frac{1}{n}$	log k_F	R^2
30	9.60	3.50×10^5	0.995	0.28	0.81	0.790
40	9.61	5.19×10^5	0.992	0.27	0.85	0.782
50	9.62	8.49×10^5	0.998	0.27	0.90	0.780

The Langmuir equation indicates that the adsorption energy of each molecule is the same, the surface sites of the adsorbent are independent, adsorption only takes place on some surface sites and there is no interaction between molecules. The maximal vanadium adsorption capacity calculated from the Langmuir model is 9.60 mg·g^{-1}, and the Langmuir constant, R^2, is 0.995. However, the Freundlich constant, R^2, is just 0.790. Thus the experimental data are better fitted to the Langmuir than the Freundlich model, which means that the active sites over the entire outer γ-CrOOH surface could be homogenous and vanadium adsorption might form a monolayer on the γ-CrOOH outer surface.

A dimensionless constant, R_L, called the 'constant separation factor' or 'equilibrium parameter', can be calculated using Equation (7) (Hall *et al.* 1966; Salehi *et al.* 2020):

$$R_L = \frac{1}{1 + K_L C_0} \tag{7}$$

where K_L is the Langmuir constant related to the adsorption capacity (L·mol^{-1}), C_0 the initial vanadium concentration (mg-V·L^{-1}). R_L can be used to estimate the affinity between the adsorbent and adsorbate. The shape of the isotherm is shown by R_L: linear ($R_L = 1$), irreversible ($R_L = 0$), unfavorable ($R_L > 1$) and favorable ($0 < R_L < 1$) (Hall *et al.* 1966). The value of R_L (1.20×10^{-4} to 2.91×10^{-4}) is in the range 0 to 1, showing that γ-CrOOH will adsorb vanadium. The Freundlich parameter $\frac{1}{n} = 0.28$ ($0.1 < \frac{1}{n} < 1.0$) also indicates that vanadium adsorption onto γ-CrOOH is favorable (Kara & Demirbel 2012).

CONCLUSIONS

In this work, a mesoporous amorphous γ-CrOOH with a specific surface and pore volume of 99.2 m^2·g^{-1} and 0.2 cm^3·g^{-1} was prepared by hydrogen reduction of K_2CrO_4. It was used as an adsorbent for vanadium from wastewater. In batch mode studies, the adsorption of vanadium onto γ-CrOOH was found to be highly dependent on the solution pH, adsorbent dosage, temperature, and adsorption time.

When an adsorbent dosage ratio of 60:1 was applied to a solution containing 300 mg-V·L^{-1}, under initial conditions pH = 2 at T = 30 °C, more than 99% of the vanadium was removed after 3.0 hours. The residual vanadium concentration in the effluent after 10.0 hours was below 0.75 mg-V·L^{-1}, which meets the vanadium discharge standard (<1.0 mg·L^{-1}, China).

Studies on the effect of common co-existing ions showed that γ-CrOOH can remove vanadium from real effluents efficiently.

The adsorption kinetics data fit well with the pseudo-second-order equation, indicating that the limiting factor for vanadium adsorption ions onto γ-CrOOH was chemisorption. The Langmuir model – with $R^2 = 0.995$ – fitted the experimental data better than the Freundlich model, indicating that the active sites over the γ-CrOOH outer surface could be homogenous, with vanadium adsorption occurring on surface sites to form a monolayer and no interaction between the molecules.

ACKNOWLEDGEMENTS

This work was financially supported by the National Natural Science Foundation of China (U1903131).

DATA AVAILABILITY STATEMENT

All relevant data are included in the paper or its Supplementary Information.

REFERENCES

Bai, Y. L., Xu, H. B., Zhang, Y. & Li, Z. H. 2006 Reductive conversion of hexavalent chromium in the preparation of ultrafine chromia powder. *Journal of Physics and Chemistry of Solids* **67**(12), 2589–2595. https://doi.org/10.1016/j.jpcs.2006.07.018.

Cheng, X., Ye, J. X., Sun, D. Z. & Chen, A. Y. 2011 Influence of synthesis temperature on phosphate adsorption by Zn-Al layered double hydroxides in excess sludge liquor. *Chinese Journal of Chemical Engineering* **19**(3), 391–396. https://doi.org/10.1016/S1004-9541(09)60226-3.

Hall, K. R., Eagleton, L. C., Acrivos, A. & Vermeulen, T. 1966 Pore-and solid-diffusion kinetics in fixed-bed adsorption under constant-pattern conditions. *Industrial & Engineering Chemistry Fundamentals* **5**(2), 212–223. https://doi.org/10.1021/i160018a011.

Ho, Y. S., Ng, J. C. Y. & Mckay, G. 2000 Kinetics of pollutant sorption by biosorbents: review. *Separation and Purification Methods* **29**(2), 189–232. https://doi.org/10.1081/SPM-100100009.

Hong, M., Yu, L. Y., Wang, Y. D., Zhang, J., Chen, Z. W., Dong, L., Zan, Q. J. & Li, R. L. 2019 Heavy metal adsorption with zeolites: the role of hierarchical pore architecture. *Chemical Engineering Journal* **359**, 363–372. https://doi.org/10.1016/j.cej.2018.11.087.

Hu, J., Wang, X. W., Xiao, L. S., Song, S. R. & Zhang, B. Q. 2009 Removal of vanadium from molybdate solution by ion exchange. *Hydrometallurgy* **95**(3–4), 203–206. https://doi.org/10.1016/j.hydromet.2008.05.051.

Kara, A. & Demirbel, E. 2012 Kinetic, isotherm and thermodynamic analysis on adsorption of Cr (VI) ions from aqueous solutions by synthesis and characterization of magnetic-poly (divinylbenzene-vinylimidazole) microbeads. *Water Air and Soil Pollution* **223**(5), 2387–2403. https://doi.org/10.1007/s11270-011-1032-1.

Khalid, M. K., Leiviskä, T. & Tanskanen, J. 2017 Properties of vanadium-loaded iron sorbent after alkali regeneration. *Water Science and Technology* **76**(10), 2672–2679. https://doi.org/10.2166/wst.2017.434.

Kong, X. R., Chen, J. H., Tang, Y. J., Lv, Y., Chen, T. & Wang, H. T. 2020 Enhanced removal of vanadium (V) from groundwater by layered double hydroxide-supported nanoscale zerovalent iron. *Journal of Hazardous Materials* **392**, 122392. https://doi.org/10.1016/j.jhazmat.2020.122392.

Li, P., Zheng, S. L., Qing, P. H., Chen, Y. A., Tian, L., Zheng, X. D. & Zhang, Y. 2014 The vanadate adsorption on a mesoporous boehmite and its cleaner production application of chromate. *Green Chemistry* **16**(9), 4212–4222. https://doi.org/10.1039/c4gc00897a.

Liang, S. T., Zhang, H. L. & Xu, H. B. 2020 Preparation of hexagonal and amorphous chromium oxyhydroxides by facile hydrolysis of K_xCrO_y. *Transactions of Nonferrous Metals Society of China* **30**(5), 1397–1405. https://doi.org/10.1016/S1003-6326(20)65305-5.

Naeem, A., Westerhoff, P. & Mustafa, S. 2007 Vanadium removal by metal (hydr)oxide adsorbents. *Water Research* **41**(7), 1596–1602. https://doi.org/10.1016/j.watres.2007.01.002.

Padilla-Rodríguez, A., Hernandez-Viezcas, J. A., Peralta-Videa, J. R., Gardea-Torresdey, J. L., Perales-Pérez, O. & Roman-Velázquez, F. R. 2015 Synthesis of protonated chitosan flakes for the removal of vanadium (III, IV and V) oxyanions from aqueous solutions. *Microchemical Journal* **118**, 1–11. https://doi.org/10.1016/j.microc.2014.07.011.

Peng, H., Liu, Z. H. & Tao, C. Y. 2017 Adsorption kinetics and isotherm of vanadium with melamine. *Water Science and Technology* **75**(10), 2316–2321. https://doi.org/10.2166/wst.2017.094.

Ratnasamy, P. & Leonard, A. J. 1972 Structural evolution of chromia. *Journal of Physical Chemistry* **76**(13), 1838–1843. https://doi.org/10.1021/j100657a009.

Salehi, S., Mandegarzad, S. & Anbia, M. 2020 Preparation and characterization of metal organic framework-derived nanoporous carbons for highly efficient removal of vanadium from aqueous solution. *Journal of Alloys and Compounds* **812**, 152051. https://doi.org/10.1016/j.jallcom.2019.152051.

Sharififard, H. & Rezvanpanah, E. 2021 Ultrasonic-assisted synthesis of SiO_2 nanoparticles and SiO_2/chitosan/Fe nanocomposite and their application for vanadium adsorption from aqueous solution. *Environmental Science and Pollution Research* **28**(9), 11586–11597. https://doi.org/10.1007/s11356-020-11346-2.

State Administration for Quality Supervision, Inspection and Quarantine, Ministry of Environmental Protection, People's Republic of China 2011 *Discharge Standard of Pollutants for Vanadium Industry: GB 26452-2011*. Environmental Science Press of China, Beijing, China.

Thommes, M., Kaneko, K., Neimark, A. V., Olivier, J. P., Rodriguez-Reinoso, F., Rouquerol, J. & Sing, K. S. W. 2015 Physisorption of gases, with special reference to the evaluation of surface area and pore size distribution (IUPAC technical report). *Pure and Applied Chemistry* **87**(9–10), 1051–1069. https://doi.org/10.1515/pac-2014-1117.

Wang, L., Niu, Z. P. & Zhu, X. B. 2021 Recovery of iron by jarosite crystallization and separation of vanadium by solvent extraction with extractant 7101 from titanium white waste liquid (TWWL). *Water Science and Technology* **83**(8), 2025–2037. https://doi.org/10.2166/wst.2021.114.

Xie, X. L., Zhao, X. N., Luo, X., Su, T. M., Zhang, Y. Q., Qin, Z. Z. & Ji, H. B. 2020 Mechanically activated starch magnetic microspheres for Cd(II) adsorption from aqueous solution. *Chinese Journal of Chemical Engineering*. https://doi.org/10.1016/j.cjche.2020.06.003.

Xiong, P., Zhang, Y. M., Bao, S. X. & Huang, J. 2018 Precipitation of vanadium using ammonium salt in alkaline and acidic media and the effect of sodium and phosphorus. *Hydrometallurgy* **180**, 113–120. https://doi.org/10.1016/j.hydromet.2018.07.014.

Yang, J., Martens, W. N. & Frost, R. L. 2011 Transition of chromium oxyhydroxide nanomaterials to chromium oxide: a hot-stage Raman spectroscopic study. *Journal of Raman Spectroscopy* **42**(5), 1142–1146. https://doi.org/10.1002/jrs.2773.

Yang, M. G., Wang, X. W., Meng, Y. Q. & Wang, M. Y. 2020 Recovery of chromium from vanadium precipitated solution by precipitation with lead salt and leaching with sodium carbonate. *Hydrometallurgy* **198**, 105501. https://doi.org/10.1016/j.hydromet.2020.105501.

Yu, Y. Q. & Yang, J. Y. 2019 Oral bioaccessibility and health risk assessment of vanadium (IV) and vanadium (V) in a vanadium titanomagnetite mining region by a whole digestive system in-vitro method (WDSM). *Chemosphere* **215**, 294–304. https://doi.org/10.1016/j.chemosphere.2018.10.042.

First received 23 April 2021; accepted in revised form 24 July 2021. Available online 9 August 2021